THE PENNSYLVANIA STATE UNIVERSITY
SCHREYER HONORS COLLEGE

DEPARTMENT OF CHEMICAL ENGINEERING

FLUX-DEPENDENT TRANSMISSION OF RNA THROUGH THE USE OF PRECONDITIONING WITH ULTRAFILTRATION MEMBRANES

SCOTT BERMAN
SUMMER 2018

A thesis
submitted in partial fulfillment
of the requirements
for a baccalaureate degree
in Chemical Engineering
with honors in Chemical Engineering

Reviewed and approved* by the following:

Dr. Andrew Zydney
Bayard D. Kunkle Chair, Professor of Chemical Engineering
Thesis Supervisor

Dr. Michael Janik
Professor of Chemical Engineering
Honors Adviser

* Signatures are on file in the Schreyer Honors College.

ABSTRACT

Recent studies of DNA ultrafiltration have demonstrated the potential for vastly improving the performance of membrane-based DNA separations by controlling the pore morphology to pre-stretch the DNA prior to filtration through the very small pores of the ultrafiltration membrane. This pre-stretching leads to an increase in DNA transmission and a reduction in membrane fouling. The objective of this thesis was to determine whether a similar approach could be used to enhance the performance of RNA ultrafiltration given the growing interest in RNA-based therapies. Experiments were performed in a stirred ultrafiltration cell using polyethersulfone Biomax membranes. Data were obtained with asymmetric membranes with the flow in either the normal (tight side facing the feed) or reverse orientations as well as with composite membrane structures created by placing a symmetric 0.22 μm pore size Durapore membrane on top of a small pore size ultrafiltration membrane. Transmission through the 100 kDa nominal molecular weight cutoff membrane was very high in both orientations, reflecting the smaller size and greater flexibility of RNA compared to DNA. RNA transmission through the 30 kDa membrane was much greater when operated with the reverse orientation, although it was not possible to clearly determine if this increase in transmission was due to pre-stretching of the RNA or to concentration polarization effects in the support structure. The results do suggest that the ultrafiltration performance for RNA separations can potentially be enhanced by controlling the underlying pore morphology of the membrane.

TABLE OF CONTENTS

LIST OF FIGURES

ACKNOWLEDGEMENTS

I would like to begin by expressing my utmost gratitude and thanks to my thesis adviser, my mentor throughout the process of composing my thesis, and my former professor, Dr. Zydney. Dr. Zydney truly went above and beyond to ensure I was able to finish my thesis on time. No matter how much I failed to follow through on certain responsibilities he was there for me to help and help me through. All I ever received from Dr. Zydney was positive reinforcement, encouragement, and help which I am truly grateful for.

I would next like to thank my parents without whom I certainly would have given up on graduating with Honors. It was from their "nudging" that I decided to finish what I started.

The last person I would like to thank is Ivan Manzano, who guided me in my research in the lab. He was incredibly patient with me and never hesitated to take extra time to ensure that I understood everything I was working on. I wish him the best of luck on his Ph.D.

1. Introduction

The discovery of short interfering (siRNA) and micro RNA (miRNA) nearly 20 years ago by Fire and colleagues has led to a deepened interest in nucleic acid therapies as an alternative to traditional methods of treating diseases and other genetic disorders [1]. siRNA-based therapies have recently become one of the most clinically advanced platforms for the development of RNA drugs with the potential to treat currently incurable diseases like cancer and AIDS [1]. RNA can potentially be used to suppress or regulate gene expression simply by designing a complementary sequence to the target mRNA. The specificity of RNA interactions is particularly attractive for the development of personalized medicine in cancer therapy [2]. In addition, recent advances in CRISPR technology, an RNA guided gene-editing tool, have placed RNA-based therapeutics at the center of what could be a watershed moment in biomedical science and personalized medicine [3]. CRISPR CAS-9, along with siRNAs, miRNAs, and antisense oligonucleotides, have the potential to revolutionize disease and cancer treatment [2]. There is thus a rapidly growing demand for fast and reliable commercial techniques for large-scale purification of RNA [3].

Many of the current techniques used to isolate and purify RNA molecules have significant limitations, particularly for large-scale commercial production of these new biotherapeutics. This includes the use of chloroform extraction, chromatographic methods, and isolation on isopycnic gradients [4].

Membrane separation processes offer a potentially attractive alternative that addresses some of the key drawbacks and limitations of current methods for RNA purification. Ultrafiltration

avoids the use of any additional chemicals, it is easily scalable from bench-top to commercial manufacturing, and it can be operated continuously with high productivity. Although a number of studies have examined the behavior of ultrafiltration processes for purification of DNA and specific plasmid DNA isoforms, there has been little to no work on RNA ultrafiltration. Although RNA and DNA are both nucleic acids, DNA is much longer (larger number of base pairs) and the double helix DNA structure provides very different physical properties than the single-stranded RNA molecules.

Previous studies of DNA ultrafiltration have demonstrated that the large DNA molecules pass through the narrow membrane pores by first elongating in the converging flow field above the pores. There is thus a critical filtrate flux for plasmid transmission, with the plasmids being almost entirely rejected by the membrane below the critical flux due to the lack of elongation [5]. These studies have generally shown little to no dependence of plasmid retention on the DNA size, with the larger plasmids having more time to elongate as they approach the pore. This behavior is in good agreement with predictions of scaling models developed to describe the elongation of single polymer chains during passage through isolated small pores [6].

One of the challenges in DNA ultrafiltration is membrane fouling due to plasmids becoming trapped at the entrance to the pores. Li et al. [7] showed that DNA fouling could be significantly reduced by pre-stretching (or pre-elongating) the DNA by first passing the DNA through a larger pore size filter (approximately 0.2 μm pore size) prior to transmission through the very small pores of the ultrafiltration membrane. In addition, pre-stretching the DNA significantly increased DNA transmission at a given value of the filtrate flux [7]. There have been no previous studies of the effects of pre-stretching on the ultrafiltration behavior of RNA.

The objective of this study was to extend the previous work on DNA to the ultrafiltration of RNA and to specifically investigate whether pre-conditioning can be used to improve the performance of membrane systems for RNA purification.

2. Materials and Methods

Stirred (and unstirred) cell ultrafiltration experiments were conducted using Biomax polyethersulfone membranes (MilliporeSigma, Bedford, MA) with nominal molecular weight cutoffs of 30 and 100 kDa. These membranes are asymmetric: they have a thin skin with the selective pores on top of a macroporous support structure that provides the membrane with its mechanical stability. These membranes are traditionally used with the thin skin facing the feed; thus, the permeate flows through the smallest pores before entering the support structure (regular orientation). It is also possible to use these membranes in the reverse orientation, with the flow passing first through the larger pores in the substructure before reaching the selective (nanometer-scale) pores in the thin skin.

Membrane discs (22.8 mm diameter) were cut from large flat sheets using a specially designed membrane cutting device. These membranes were pre-wet by soaking in 90% isopropyl alcohol (IPA) for a minimum of 45 minutes prior to use in the filtration experiments. The membranes were then flushed with water to remove any residual IPA. Limited experiments were also performed with symmetric 0.22 μm pore size Durapore hydrophilic polyvinylidene fluoride (PVDF) membranes placed immediately above (upstream) of a Biomax membrane. All membranes were flushed with at least 40 mL of buffer solution before the RNA ultrafiltration.

Buffer solutions were prepared by 100x dilution of Tris-EDTA (TE) concentrate with DI water obtained from a Barnstead International Nanopure water purification system (Thermo Scientific, IL). Solutions were prefiltered through 0.2 µm pore size Supor® 200 disc filters obtained from Pall Corporation (Port Washington, NY) to remove any particulate matter or undissolved salt.

Experiments were conducted with Torula Yeast RNA, obtained from Sigma Aldrich and stored frozen at -80ºC. The concentrations of the stock solutions of RNA were determined by a Nanodrop 1000 spectrophotometer (Thermo Scientific) based on the absorbance at 485 and 535 nm; the RNA was checked periodically for degradation by UV-VIS Absorbance at 260 nm. A small amount of stock solution was thawed and diluted with TE buffer immediately prior to use in the ultrafiltration experiments.

a. Ultrafiltration Experiments

Sieving experiments were conducted using a 15 mL stirred ultrafiltration cell (MilliporeSigma) placed on top of a magnetic stir plate. The cell was initially filled with buffer and then connected to a polycarbonate feed reservoir which was pressurized with compressed air. After measuring the permeability (see below) the stirred cell and feed reservoir were emptied and filled with an RNA solution, the stirrer was set to the lowest possible stirring speed, and the system was allowed to equilibrate for approximately 1 minute (without any filtration). A small sample (approximately 500 µL) was taken directly from the stirred cell to evaluate the feed concentration. The stirred cell was then reconnected to the feed reservoir, and the feed pressure was set to the desired value to start the ultrafiltration experiment. RNA sieving data were obtained over a range of filtrate fluxes from 25 to 250 µm/s, corresponding to pressures between 1-14 psig as measured by a digital differential pressure gauge. Prior to taking a permeate sample

at each pressure, approximately 4 mL of permeate were allowed to pass through the membrane to wash out the dead volume beneath the membrane and ensure steady state operation. A permeate sample of at least 500 µL was collected, the stirred cell was disconnected from the feed reservoir, and a post-sieving sample of 500 µL was taken directly from the stirred cell. All experiments were performed at room temperature (22-25ºC).

b. Membrane Permeability (Lp)

Prior to each experiment, the integrity of the membrane permeability was evaluated to ensure that the membrane was intact and properly situated in the stirred cell. The membrane was first flushed with 40 mL of buffer at a pressure of approximately 2.5 psig. The filtrate flux was then evaluated by timed collection at pressures of 2.0, 4.0, 6.0, and 8.0 psig, with the permeability determined from Equation 1:

$$L_p = J\mu/\Delta P \qquad (1)$$

where J is the filtrate flux (in m^3 filtrate per second normalized by the membrane area in m^2) and µ is the solution viscosity. Membranes were discarded if the permeability was not within 10% of the expected value for the given membrane ($L_p = 1.1 \times 10^{12}$ m for the Biomax 30 kDa and $L_p = 2.3 \times 10^{12}$ m for the Biomax 100 kDa). The calculated values of the permeability were also used to determine the required pressure to achieve a desired filtrate flux.

c. Quantitative Assay

RNA concentrations were determined using the Quant-iT RiboGreen RNA Assay Kit (Life Technologies, Carlsbad, CA). The RiboGreen working solution was prepared by 2000x dilution

of the concentrated dye with DI water and 20x TE buffer provided by the manufacturer. 100 µL of the sample and working solution were loaded into separate wells of a 96-well microplate (VWR, Philadelphia, PA). Each sample was run in duplicate. Due to RiboGreen's sensitivity to light, all procedures were performed with the lights off. The microplate was inserted into a TECAN GENiosFL microplate reader set to 25ºC, mixed by orbital shaking for 60 seconds, and allowed to settle for 30 seconds. A calibration curve was constructed by measuring the fluorescence intensity for samples of known concentration loaded on the microplate.

d. Concentration Polarization Model

The experimental data for RNA transmission were used to evaluate the observed sieving coefficient (S_o), defined as the ratio between the RNA concentration in the permeate (C_p) to that in the bulk solution (C_b):

$$S_o = \frac{C_p}{C_b} \qquad (2)$$

Recent work by Manzano and Zydney [8] has shown that the dependence of the RNA sieving coefficient on the ultrafiltration flux can be described by the concentration polarization model, which accounts for the accumulation of retained RNA in the solution immediately upstream of the membrane. The RNA concentration (C) in the boundary layer above the membrane is evaluated using a simple one-dimensional mass balance:

$$-JC - D\frac{\partial C}{\partial Y} = N_S = -JC_P \qquad (3)$$

where J is the filtrate flux, y is the distance measured perpendicular to the membrane surface, D is the RNA diffusion coefficient, N_s is the RNA flux through the membrane, and C_p is the RNA concentration in the permeate solution. The filtrate flux carries RNA towards the membrane, with the RNA retention by the small pores leading to a buildup of RNA molecules at the membrane surface. The resulting concentration gradient causes back diffusion of RNA away from the membrane surface. At low flux, the rate of diffusion dominates convection so that there is negligible accumulation of RNA in the solution upstream of the membrane surface with C = C_b at all values of y. However, at high flux, the RNA begins to accumulate in the solution above the membrane, with the RNA concentration at the membrane surface becoming much larger than that in the bulk (feed) solution.

Equation (3) can be integrated across the concentration polarization boundary layer, with the RNA concentration at the membrane surface, y = 0, equal to C_W, and the RNA concentration at the edge of the boundary layer, y = δ, equal to C_b. The resulting equation can be reorganized to solve for the sieving coefficient:

$$S_o = \frac{S_a}{(1-S_a)exp(-J/k_m)+S_a} \qquad (4)$$

The bulk mass transfer coefficient, k_m, has been set equal to D/δ. The mass transfer coefficient is a function of the RNA diffusion coefficient, the geometry of the stirred cell, and the stirrer speed. $S_a = C_p/C_w$ is the actual sieving coefficient, which describes the fractional transmission of the RNA through the membrane (ratio of permeate concentration to the concentration in the solution at the upstream surface of the membrane).

3. Results and Analysis

Fig. 1 shows a typical calibration curve used to evaluate the RNA concentration. The fluorescence intensity was measured using the RiboGreen assay for samples with RNA concentrations up to 600 ng/ml for Torula Yeast RNA samples with known concentration. The data are highly linear, with a correlation coefficient of $R^2 = 0.994$. RNA calibration curves were constructed for each experiment to account for any variations in the fluorescent dye, the ambient temperature, or the microplate reader.

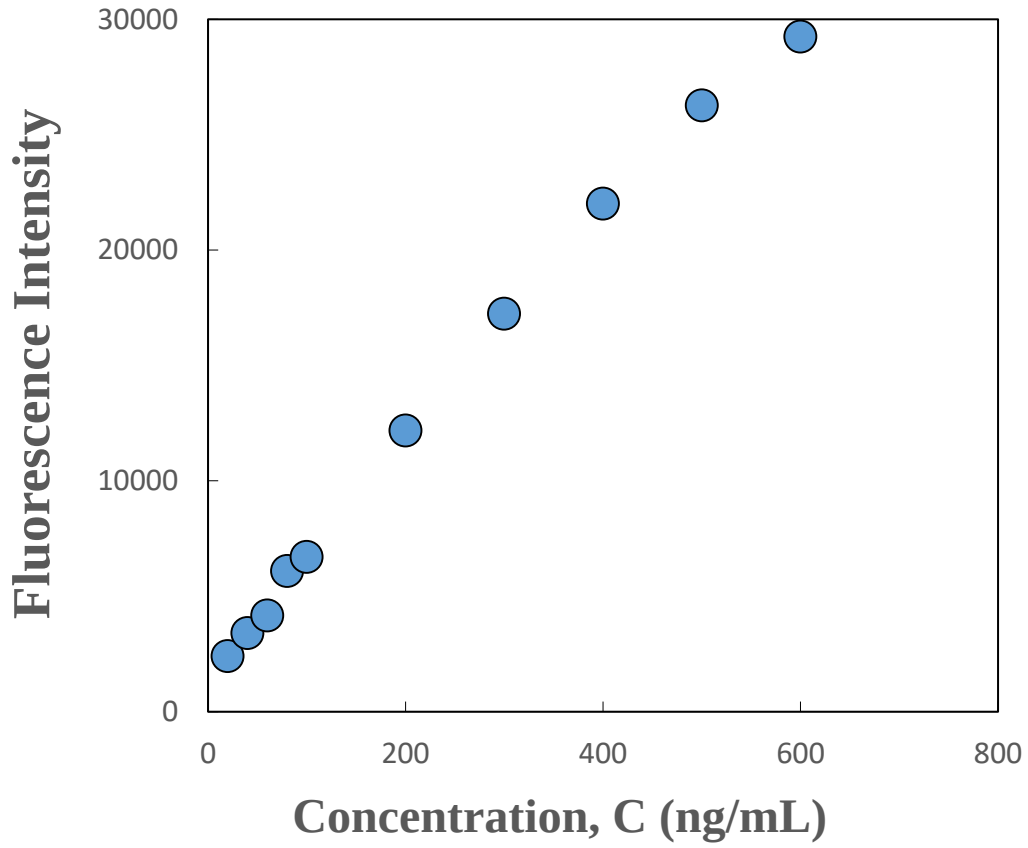

Figure 1 — Typical calibration curve for RNA concentrations using RiboGreen assay

Figure 2 shows results from a preliminary experiment. S_o was very low at the beginning of the experiment, but tended to increase over time as the filtrate flux was increased. Similar results are

described by Manzano and Zydney [8] and were shown to be due to RNA adsorption to the new membrane at the start of the experiment. This is shown explicitly in Figure 3 which compares data for a new (Non-Saturated) membrane with that for a membrane that was pre-adsorbed with RNA (Pre-saturated). The sieving coefficient through the Pre-saturated membrane is much higher for the first data point (at low flux) but the transmission through the two membranes are nearly the same at the end of the experiment (data at high flux).

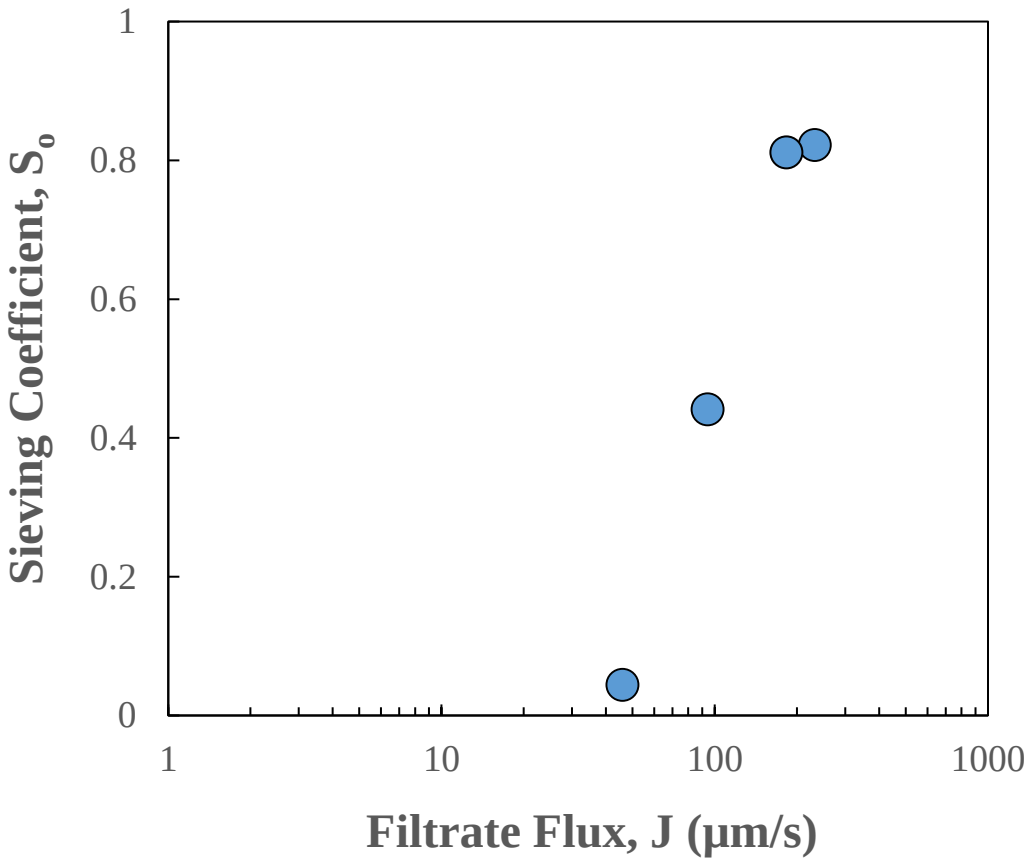

Fig 2 — Sieving coefficient versus flux for an early experiment using a clean (not pre-saturated) 100 kDa membrane in the normal orientation

It was hypothesized that RNA adsorption to the polymeric membrane was responsible for the initially low transmission, a hypothesis that was supported by a simple mass balance which showed that there was missing RNA at the start of the experiment. Thus, in all subsequent

experiments used membranes that were Pre-saturated with RNA. This pretreatment involved permeating 10 mL of a high concentration (24 µg/mL) RNA solution through the membrane at ~2 psi to saturate the membrane surface with RNA.

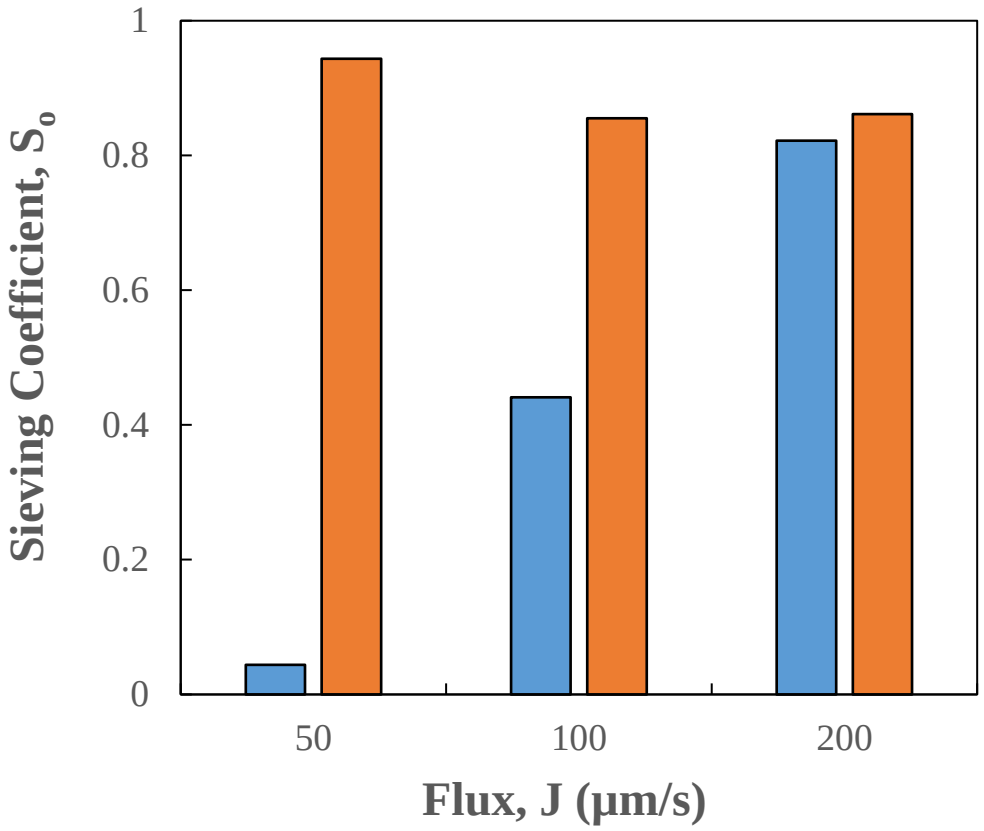

Fig 3 – Sieving coefficient versus flux for two 100 kDa Ultracel® membranes, one Non-Saturated (■) and one Pre-saturated (■) with a 24 µg/mL RNA solution. The data points at J = 50 µm/s were taken first followed by the data at 100 and 200 µm/s.

Figure 4 shows data for the observed sieving coefficient (S_o) obtained with a 0.4 µg/mL solution of the Torula yeast RNA during ultrafiltration through a pre-saturated Biomax 30 kDa membrane in the normal orientation (skin-side facing the feed). S_o was very low at low fluxes, but increased with increasing flux reaching a value of 0.33 at a filtrate flux of 100 µm/s (corresponding to 360 $L/m^2/h$). This behavior is in good agreement with predictions of the concentration polarization

model discussed earlier, with the increase in sieving coefficient arising from the increase in RNA concentration in the solution immediately upstream of the membrane surface.

The solid curve in Figure 4 shows the calculated values of the observed sieving coefficient given by the concentration polarization model using the best fit values of the actual sieving coefficient, $S_a = 3.0 \times 10^{-5}$, and the mass transfer coefficient, $k_m = 10.2$ µm/s, both determined by minimizing the sum of the squared residuals between the model (Equation 4) and the data. The model calculations are in excellent agreement with the data over the full range of filtrate flux, providing strong support for the validity of the concentration polarization model for RNA ultrafiltration under the conditions of this experiment.

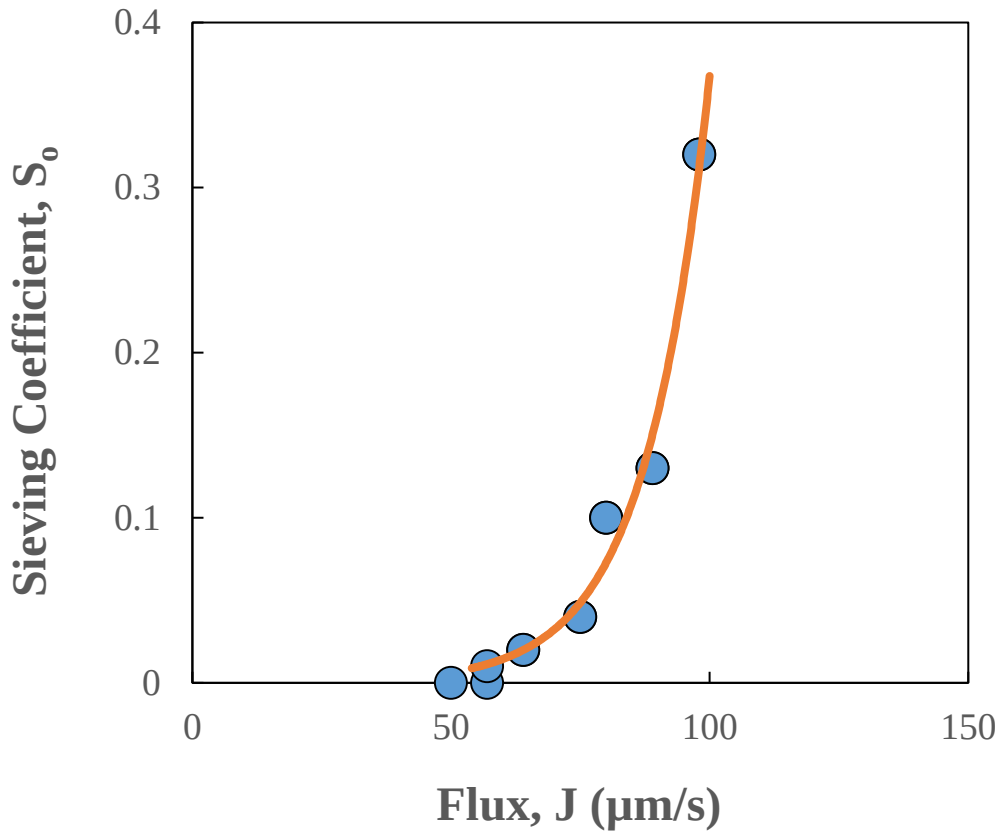

Fig 4 — RNA sieving coefficient as a function of filtrate flux (●) for the Biomax 30 kDa membrane in normal orientation. Solid curve is the best fit to the concentration polarization model (Equation 4).

Figure 5 shows corresponding data obtained for RNA ultrafiltration through a single smaller pore size Biomax 30 kDa membrane in both the normal and reverse orientations. The results were obtained with a single membrane, first with the skin-side up (normal) and then with the skin-side facing away from the feed (reverse). The RNA sieving coefficients were much higher when the membrane was oriented with the skin-side down, with the sieving coefficient remaining well above 0.5 for all values of the filtrate flux with only a very weak dependence on the flux. In contrast, RNA transmission through the membrane in the normal orientation was essentially zero for filtrate flux below 40 μm/s, increasing to only $S_o = 0.33$ at J = 94 μm/s.

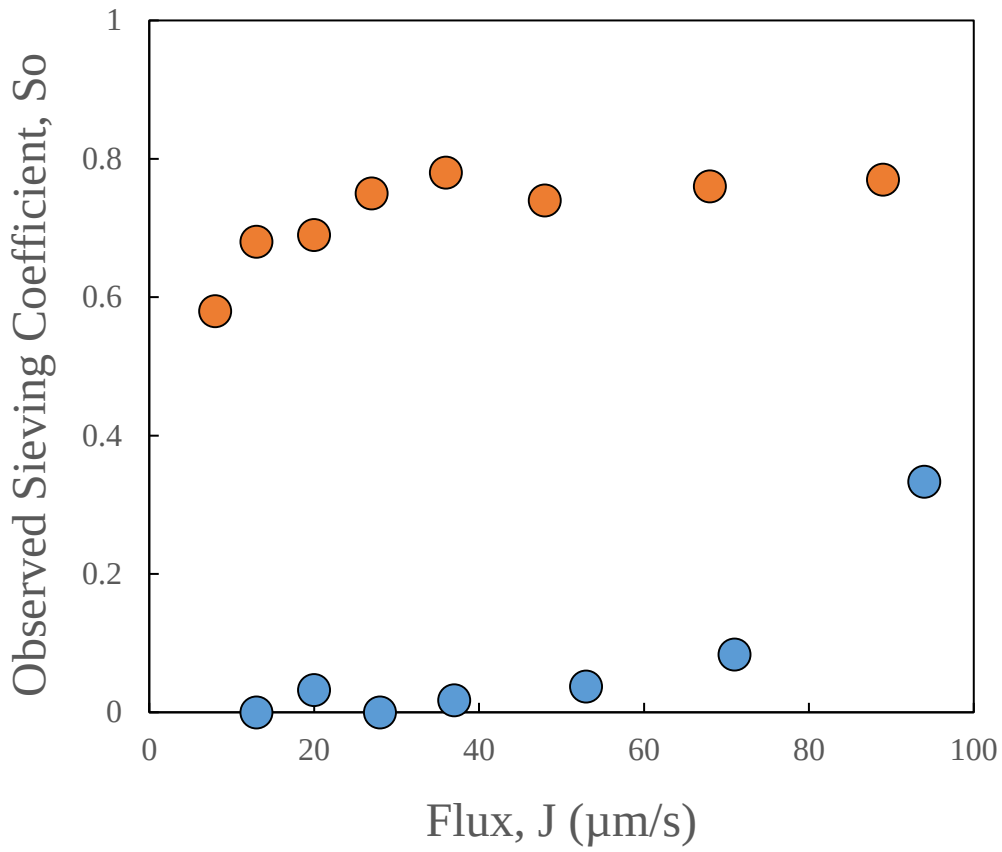

Fig 5 — RNA sieving coefficient as a function of filtrate flux for a single Biomax 30 kD in the normal (●) and reverse (●) orientations.

The RNA sieving coefficient data in the normal orientation have been replotted in Figure 6 using a linearized form of the concentration polarization model:

$$ln\left[\frac{1}{S_o}-1\right]=ln\left[\frac{1}{S_a}-1\right]-\frac{J_v}{k_m} \qquad (5)$$

Equation (5) is developed directly from Equation (4) by solving explicitly for the flux. Note that the first few points (at very low flux) were excluded from the plot since the very small values of S_o give large uncertainties in the sieving function on the left-hand side of Equation (5). The data

are highly linear when plotted in this fashion, again confirming the validity of the concentration polarization model for RNA ultrafiltration with the membrane oriented with the skin-side up. The mass transfer coefficient can be evaluated directly from the slope of the data in Figure 6 giving k_m = 10.9 μm/s, which is in good agreement with the best fit value calculated directly from the data in Figure 5 (for a separate membrane). The actual sieving coefficient can be calculated from the y-intercept in Figure 6 giving $S_a = 1.8x10^{-3}$ which is noticeably larger than the value determined from the data in Figure 3 ($S_a = 3.0 \times 10^{-5}$). This discrepancy may simply reflect the inherent variability between membranes. However, it should also be noted that there is considerable uncertainty in the calculated values of the actual sieving coefficient determined from the slope due to the difficulty in accurately evaluating the very small values of the observed sieving coefficient at low filtrate flux. For example, a shift in the observed sieving value at a flux of 37 μm/s from $S_o = 0.017$ to $S_o = 0.010$ would lead to $S_a = 9.4 \times 10^{-4}$ based on a revised linear regression fit to the data as given by Equation (5).

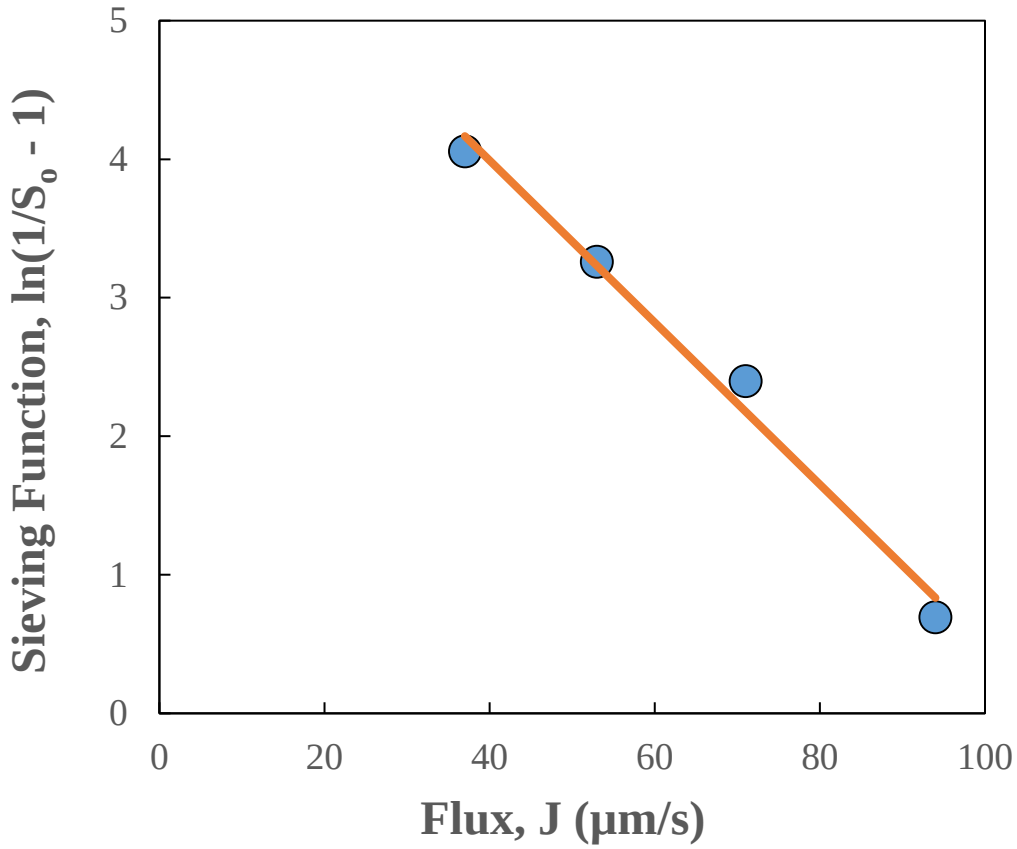

Fig 6 — Sieving function versus filtrate flux for RNA ultrafiltration through a Biomax 30 kDa membrane in the normal orientation. Solid line is linear regression fit to the data using the linearized form of the concentration polarization model (Equation 5).

Figure 7 shows a linearized plot of the RNA sieving coefficient data for the Biomax 30 kDa membrane in the reverse orientation (data from Figure 5). In sharp contrast to the results in Figure 6, the data do not appear linear when plotted in this fashion, demonstrating that the RNA transmission behavior through the membrane in the reverse orientation cannot be accurately described by the concentration polarization model.

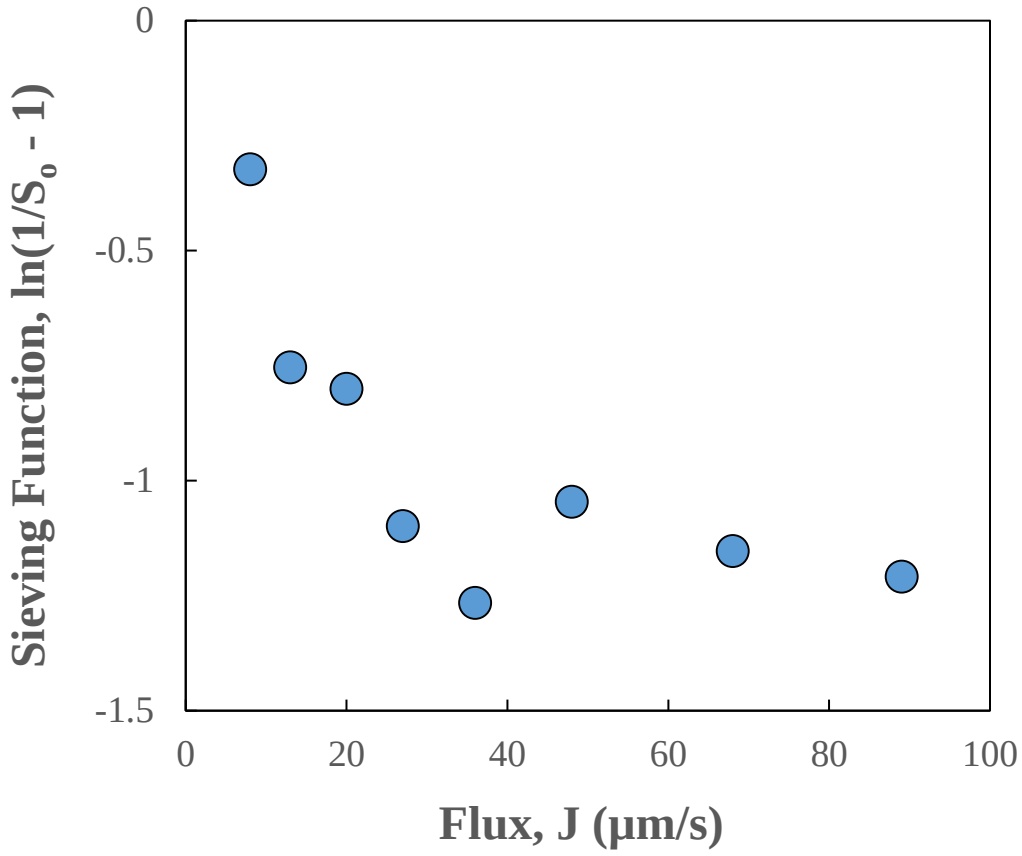

Fig 7 — Sieving function versus filtrate flux for RNA ultrafiltration through a Biomax 30 kDa membrane in the reverse orientation.

The high RNA transmission in the reverse orientation is likely related to the asymmetric pore structure of the Biomax membrane, which is shown schematically in Figure 8. In the normal orientation, the RNA directly enters the small pores at the upper surface of the membrane, leading to considerable accumulation of retained RNA at the upstream surface of the membrane (which we refer to as concentration polarization). However, when the membrane is oriented in the reverse orientation, the funnel shape allows the RNA to easily enter the large pores and pass into the depth of the membrane. In the case of DNA, Li et al. [7] showed that transport of the large DNA molecules through these funnel-shaped pores led to elongation of the highly flexible DNA, making it easier for the DNA to pass through the small pores at the exit of the filter. This

phenomenon may also occur for RNA, leading to the high transmission observed in Figure 5. Alternatively, the RNA may be retained within the membrane, just "above" the tight pores at the exit, leading to an "internal concentration polarization" phenomenon. This type of internal polarization would result in an increase in RNA transmission since the RNA concentration immediately above the tight pores would be much larger than that in the bulk (feed) solution. However, the dependence of RNA transmission on filtrate flux for this type of internal polarization may not be effectively described by the classical concentration polarization model (Equations 4 and 5), which could explain the non-linear behavior seen in Figure 7. Additional experiments would be required to more fully explain the flux behavior in the reverse orientation.

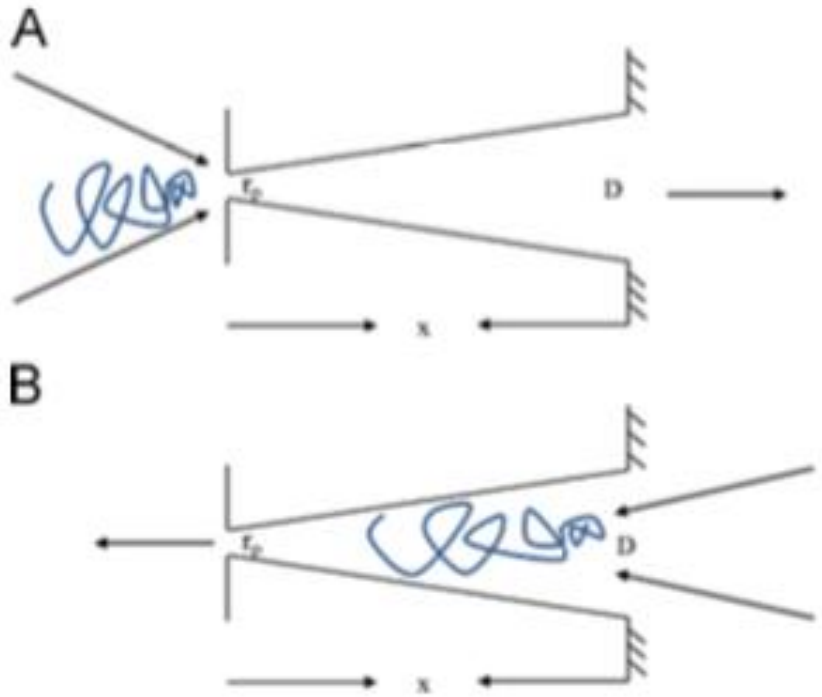

Fig 8 – Schematic diagram showing RNA transmission through an asymmetric membrane in the (A) forward and (B) reverse orientations. Reproduced from [7].

As discussed previously, RNA is much smaller than DNA. The effective size of the Torula yeast RNA used in these experiments was evaluated by dynamic light scattering (DLS), with results shown in Figure 9. The mean hydrodynamic radius of the RNA is 1.6 nm compared to the >100 nm radius determined for DNA [9]. It is very possible that the RNA is simply too small to be able elongate in the several hundred nanometer size pores within the supporting structure of the Biomax membrane.

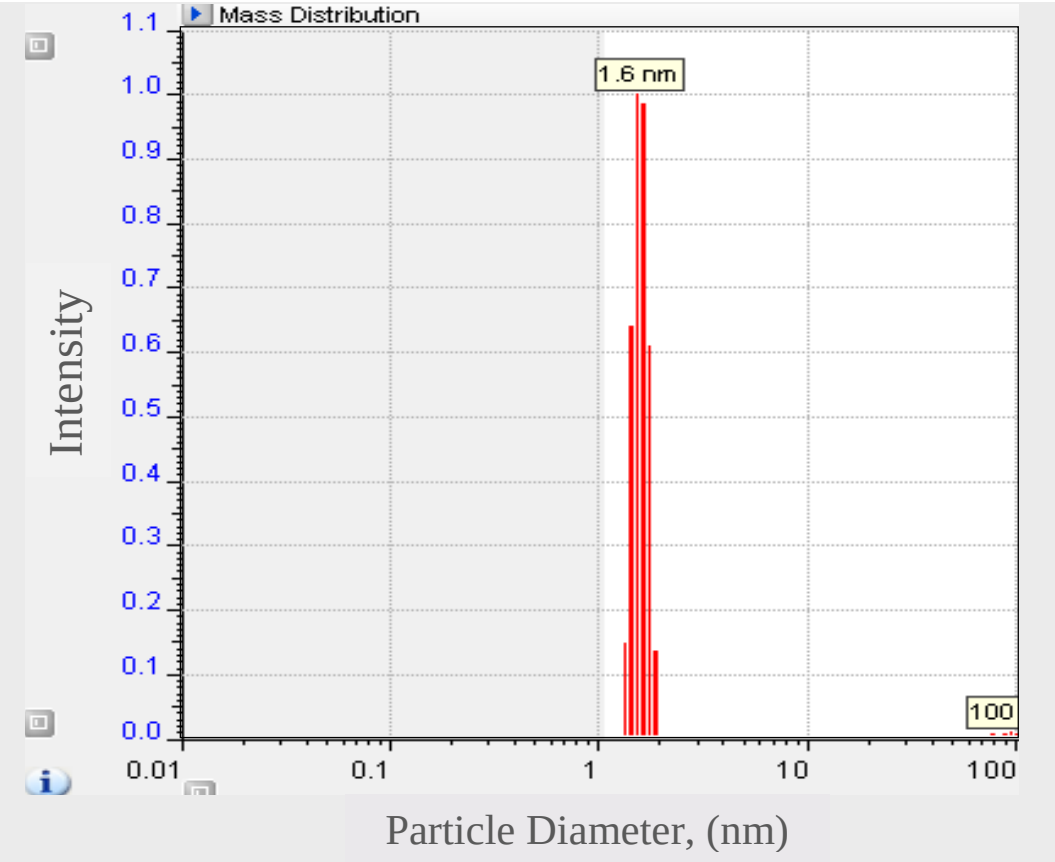

Fig 9 – Dynamic Light Scattering results for Torula Yeast RNA.

In order to obtain additional insights into the RNA ultrafiltration behavior, a series of experiments were performed with a Biomax 100 kDa membrane in both the normal and reverse

orientations. The observed sieving coefficient data for the Torula yeast RNA are shown in Figure 10 over a range of filtrate flux between 10 and 250 µm/s. The RNA transmission was very high in both membrane orientations with values between 0.8 and 1.0, essentially independent of the filtrate flux. The lack of any flux dependence is consistent with the minimal degree of concentration polarization expected with membranes that provide very low levels of RNA retention. RNA transmission was slightly higher when the membrane was in the reverse orientation, with an average value of $S_o = 0.93$ versus $S_o = 0.85$ in the normal orientation. However, given the scatter in the data, it was not possible to draw any quantitative conclusions about the effects of membrane orientation on RNA transmission through this large pore size membrane.

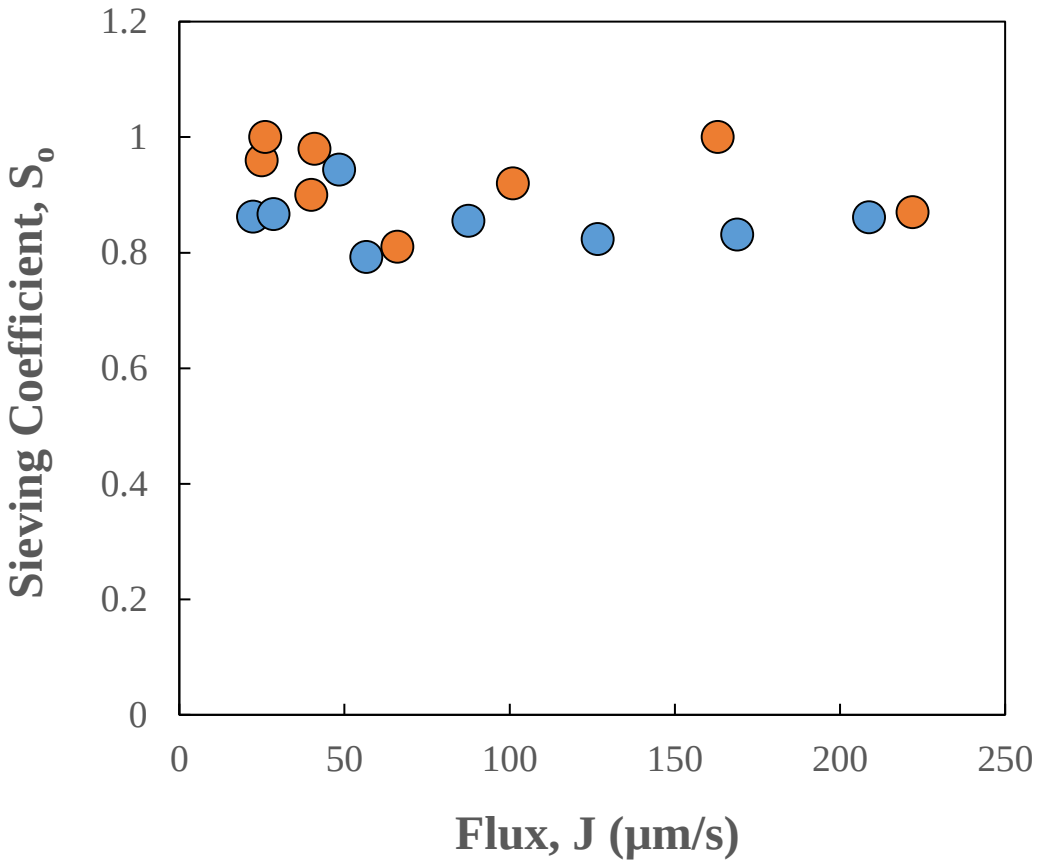

Fig 10 — RNA sieving coefficient as a function of filtrate flux for ultrafiltration through a Biomax 100 kDa membrane in the normal (●) and reverse orientations (●).

Figure 11 summarizes results for the observed sieving coefficient during RNA ultrafiltration through the Biomax 30 kDa membrane in 3 different configurations at filtrate flux values of 100 and 55 μm/s: (a) the membrane oriented with the skin-side up (normal) with stirring, (b) the membrane oriented with the skin-side down with stirring, and (c) the membrane oriented with the skin-side up but without stirring. The highest sieving coefficients are obtained with the membrane oriented with the skin-side down, with $S_o > 0.7$ at both values of the filtrate flux. The sieving coefficients obtained with the skin-side up in the presence of stirring show a strong dependence on the filtrate flux, with an 8-fold increase in value as the flux increases from J = 55 μm/s to J = 100 μm/s. The results in the unstirred system show a much smaller dependence of S_o on the filtrate flux with values at both fluxes being larger than those in the stirred system. The increase in RNA transmission in the absence of stirring is consistent with an increase in the extent of concentration polarization, with the effective mass transfer coefficient being smaller in the unstirred system. However, the very weak dependence of RNA transmission on the flux in the unstirred system is surprising. Additional experimental studies would be required to clarify this behavior.

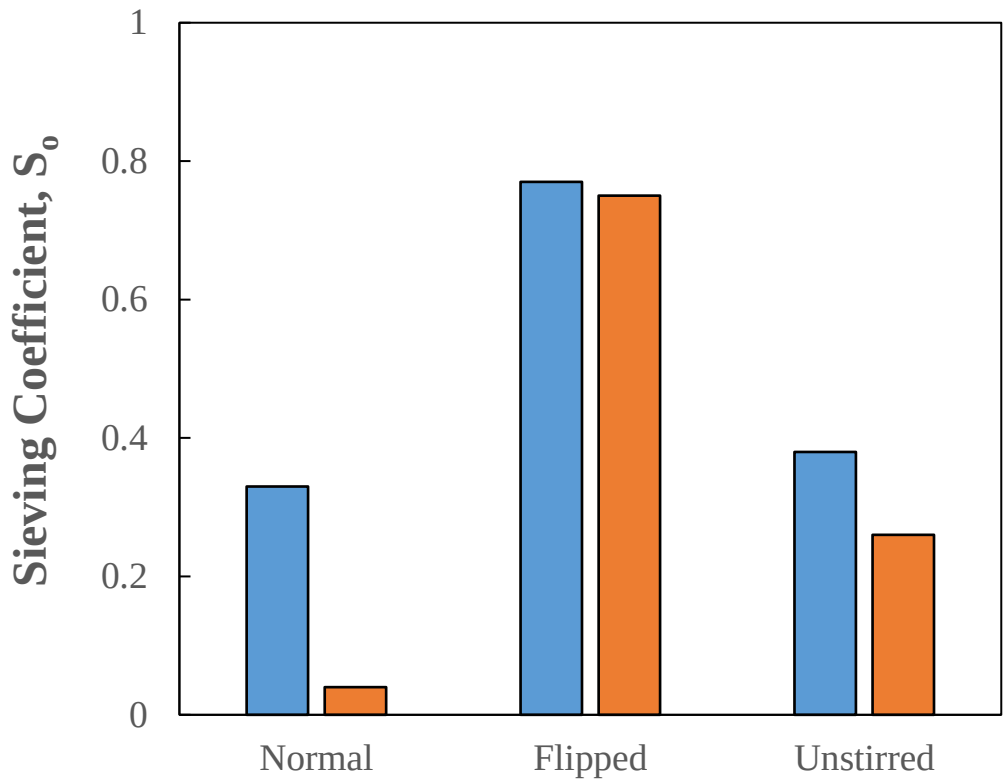

Fig 11 — Bar graph showing the RNA sieving coefficient through a Biomax 30 kDa membrane at J ≈ 100 µm/s (■) and 55 µm/s (■) in normal and reverse orientations and in the normal orientation but without any stirring.

In order to confirm that flow through the macroporous support region of the Biomax 30 kDa membrane was the cause of the enhanced RNA transmission, a sieving experiment was performed using a composite membrane structure constructed by placing a 0.2 µm pore size PVDF membrane directly on top of (before) a Biomax 30 kDa membrane, with the Biomax membrane operated in the normal orientation (skin-side up). The PVDF membrane is homogenous (uniform pore size throughout the depth) with a much larger pore size than the RNA (200 nm versus ≈2 nm for the RNA). The RNA sieving coefficient data through this composite membrane structure are shown in Figure 12. The sieving coefficients are around 0.6

for filtrate fluxes below 100 µm/s and increase to nearly 0.8 at J = 200 µm/s. Note that the RNA transmission through the Biomax 30 kDa membrane alone (data in Figure 4) remained below 0.1 for filtrate flux values as high as 80 µm/s. Thus, the presence of the 0.2 µm pore size PVDF membrane causes nearly a 10-fold increase in RNA transmission at low to moderate flux, similar to the high transmission seen with the Biomax 30 kDa membrane when operated in the reverse orientation (Figure 5). These data confirm that the increase in RNA transmission is directly due to the membrane morphology and is not related to any damage to the membrane when operated in the reverse orientation.

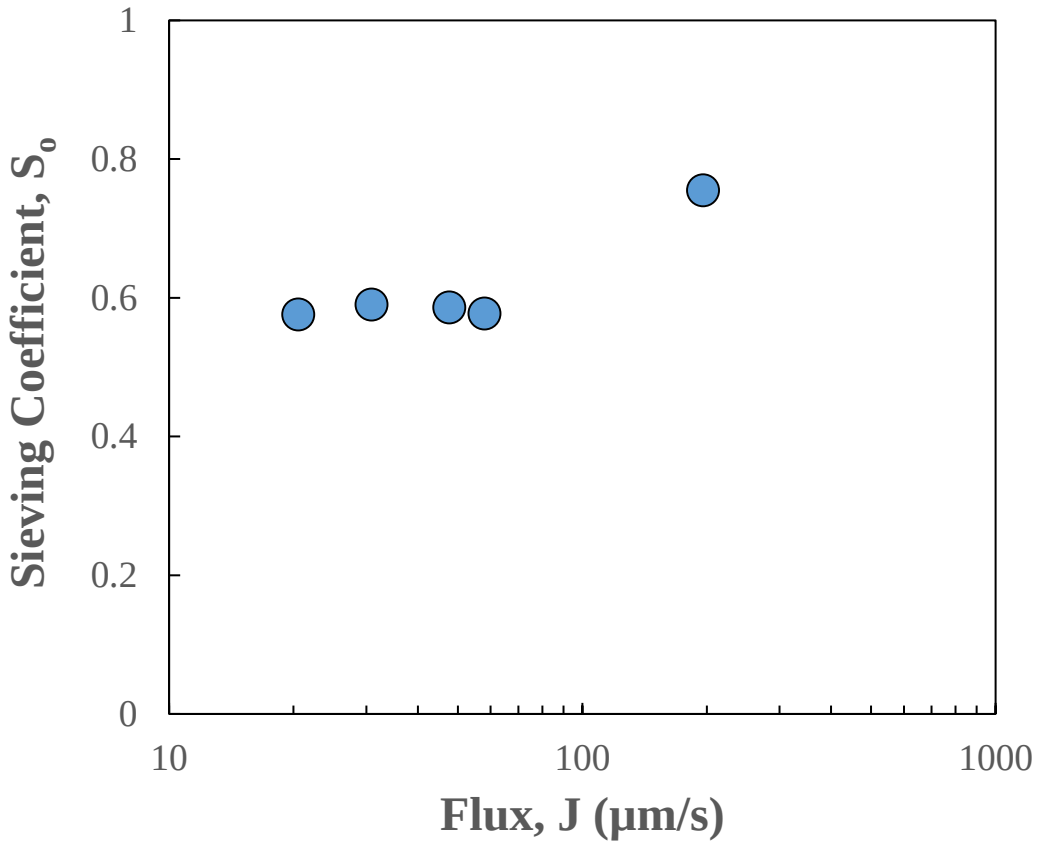

Fig 12. RNA sieving coefficient as a function of the filtrate flux for a composite membrane composed of a 0.2 µm pore size PVDF layer on top of a Biomax 30 kDa membrane oriented with the skin-side up.

Interestingly, the RNA transmission through the composite membrane structure was considerably greater than that seen in the unstirred system using the Biomax 30 kDa membrane in its normal orientation (S_o = 0.26 and 0.38 at J = 55 and 100 μm/s – data in Figure 9). This indicates that the presence of the 0.2 μm layer is more effective at increasing the RNA transmission than a "stagnant" (unstirred layer). This could simply be due to the reduced rate of RNA transport within the 0.2 μm membrane (hindered diffusion due to the presence of the pores), although it may also provide evidence for some type of flow-induced pre-elongation of the RNA within the pores of the PVDF membrane.

4. Discussion

The flux dependence of RNA transmission seen throughout this study is very similar to what has previously been seen with DNA. The RNA (and DNA) are both highly retained at low filtrate flux, with transmission increasing with increasing flux. However, DNA ultrafiltration is typically performed with a larger pore size membrane (500 kDa molecular weight cutoff), but the pores of these membranes (10 – 20 nm in radius) are much smaller than the size of the DNA (>100 nm). These studies have shown that in order for the DNA molecules to pass through the small membrane pores, they must first be elongated in the flow field above the membrane. At low filtrate flux, where the elongational flow field was very weak, the DNA was highly retained by the membrane. Although our data also show an increase in RNA transmission with increasing filtrate flux, this appears to be due to concentration polarization effects instead of RNA elongation.

Our ultrafiltration data also show no evidence of membrane fouling such as the pore blockage phenomenon observed previously with DNA [10]. During DNA ultrafiltration, there is a significant reduction in DNA transmission with time as pores are blocked by DNA molecules that become trapped at the pore entrance. There was no evidence of this type of fouling during RNA ultrafiltration, with the RNA transmission remaining constant as a function of time for as much as 40 min (data not shown). The reason for this difference is likely related to the difference in size and structure of the DNA and RNA. The plasmid DNA examined by Borujeni et al. [10] was between 3,000 and 17,000 base pairs long – if fully elongated, these DNA molecules would be 1.0 – 5.8 μm. In contrast, the RNA examined in this work is likely to be around 100 nucleotides long, with a radius of gyration (as determined by dynamic light scattering) of less than 2 nm. The much longer DNA molecules adopt a highly twisted supercoiled conformation that can easily lead to "knots" (regions of DNA that are difficult to untangle). These knots can be difficult to unwind and elongate by the hydrodynamic forces during membrane filtration, with some of these "knotted" DNA molecules becoming trapped at the entrance to the pores leading to membrane fouling. In contrast, the RNA molecules examined in this study are smaller than the effective pore size of the membrane. Thus, it is highly unlikely that the RNA will become physically trapped at the pore entrance, essentially eliminating the fouling phenomenon seen with DNA.

5. Conclusions

The experimental data presented in this thesis clearly demonstrate that the membrane pore morphology has a large effect on RNA transmission during ultrafiltration. In particular, the RNA transmission through an asymmetric Biomax 30 kDa membrane operated in the reverse

orientation (skin-side down) was as much as 10-fold (or more) larger than that through the same membrane when operated in the normal orientation. A similar increase in transmission was seen with a composite membrane composed of a large pore size membrane placed directly on top of the Biomax 30 kDa membrane, clearly demonstrating that this behavior is due to the "funnel-shaped" morphology of the pores (and not to any damage to the membrane when used in the reverse orientation).

The origin of the increase in transmission through the composite and reverse membranes is still unclear. This behavior could be due to an internal concentration polarization phenomenon, with the RNA that is retained by the tight pores in the skin accumulating within the large pores of the upper layer of the composite membrane (or of the support structure in the asymmetric membrane). However, RNA transmission through the composite and reverse membranes was actually greater than that observed through a normal Biomax 30 kDa membrane used in an unstirred system, which should have caused a very high degree of concentration polarization. Alternatively, the high degree of transmission with the reverse / composite membranes could be due to a pre-elongation of the RNA as it moves through the large pores, similar to the phenomenon seen previously with DNA. However, the much smaller size of the RNA (<2 nm) compared to the DNA would suggest that significant RNA elongation is unlikely to occur in this experimental system.

RNA transmission during ultrafiltration through the Biomax membranes in the normal orientation (skin-side up) is strongly influenced by concentration polarization effects, which causes the observed sieving coefficient to increase with increasing filtrate flux. The RNA

sieving coefficient data for the Biomax 30 kDa membrane was shown to be in excellent agreement with predictions of the concentration polarization model. In addition, RNA transmission in an unstirred system was considerably higher than that in a stirred system, with this increase in transmission due to the greater degree of concentration polarization in the absence of stirring. This behavior is considerably different than that observed previously during DNA ultrafiltration in which the DNA sieving coefficient was independent of the stirring speed. This provides further evidence for the very different behavior of RNA and DNA during ultrafiltration.

Although these studies have begun to identify some of the key factors controlling the ultrafiltration behavior of RNA in membranes with different pore morphologies, additional studies need to be conducted to fully clarify the origin of the observed phenomena. When the membrane is oriented in the reverse orientation, the funnel shape allows the RNA to easily enter the large pores and pass into the depth of the membrane. One likely reason cited for the increase in transmission is that the RNA molecules accumulate within this macroporous region. However, the RNA could easily become trapped within the membrane substructure, posing a risk of trapping other biomolecules that the ultrafiltration process is designed to remove. Further studies should be designed to evaluate this risk.

In the case of DNA, the difference in transmission observed in the forward and reverse orientations is directly related to the hydrodynamics, with the fluid flow causing plasmid elongation either in the converging flow field entering the small pores (normal orientation) or in the membrane substructure (reverse orientation). Although this seems unlikely to occur with

RNA for the reasons described above, the very high transmission and very weak dependence of the sieving coefficient on the filtrate flux when the membrane is used in the reverse orientation do not seem consistent with the effects of internal concentration polarization. Therefore, further research is required to elucidate the mechanism of transmission when the membrane is operated with "funnel-shaped" pores. In any case, this work clearly demonstrates the potential for the use of "reverse" ultrafiltration, in which the membrane is oriented skin-side down, to enhance RNA transmission through a membrane with small pores.

6. References

1. R. W. Carthew, E. J. Sontheimer, Origins and Mechanisms of MiRNAs and SiRNAs, National Center for Biotechnology Information. 136 (2009) 642-55
2. N. M. Dean, C. F. Bennett, Antisense Oligonucleotide-Based Therapeutics for Cancer, Nature, ISIS Pharmaceuticals, 2003.
3. M. Meyer, E. Wagner, Recent Developments in the Application of Plasmid DNA-Based Vectors and Small Interfering RNA Therapeutics for Cancer, Human Gene Therapy. 17 (2006) 1062–1076.
4. R. Martins, et al, Ribonucleic Acid Purification, Journal of Chromatography A, 1355 15 (2014) 1–14.
5. D.R. Latulippe, K. Ager, A.L. Zydney, Flux-dependent transmission of super- coiled plasmid DNA through ultrafiltration membranes, J. Membr. Sci. 294 (2007) 169–177.
6. D.R. Latulippe, A.L. Zydney, Elongational flow model for transmission of supercoiled plasmid DNA during membrane ultrafiltration, J. Membr. Sci. 329 (2009) 201–208.

7. Y. Li, E. E. Borujeni, A. L. Zydney, Use of preconditioning to control membrane fouling and enhance performance during ultrafiltration of plasmid DNA, J. Memb. Sci. 479 (2015) 117–122.
8. I. Manzano, A. L. Zydney, Quantitative study of RNA transmission through ultrafiltration membranes, J. Memb. Sci. 544 (2017) 272–277.
9. D. R. Latulippe, A. L. Zydney, Radius of gyration of plasmid DNA isoforms from static light scattering, Biotech. Bioeng. 107 (2010) 134-142.
10. E. E. Borujeni, A. L. Zydney, Membrane fouling during ultrafiltration of plasmid DNA through semipermeable membranes, J. Memb. Sci. 450 (2014) 189–196.

Academic Vita of Scott Berman

thescott111@gmail.com

Education
Major(s) and Minor(s): Chemical Engineering and Mathematics
Honors: Chemical Engineering

Thesis Title: Flux-Dependent Transmission of RNA Through the Use of Preconditioning With Ultrafiltration Membranes

Thesis Supervisor: Dr. Andrew Zydney

Work Experience
Date: 5/11/19
Title: Software Engineer
Institution/Company: Capital One, Mclean, VA
Supervisor's Name: Kasper Van Benten

Grants Received: Schreyer Honors College Grant

Awards: President's Freshman Award

Presentations:

Community Service Involvement:

International Education: Technion University, Haifa, Israel